WPJET1-CPR(18) 18893

S Wiesen et al.

On the role of finite grid size in SOLPS-ITER edge plasma simulations for JET H-mode discharges with metallic wall

Preprint of Paper to be submitted for publication in Proceeding of 23rd International Conference on Plasma Surface Interactions in Controlled Fusion Devices (PSI-23)

This work has been carried out within the framework of the EUROfusion Consortium and has received funding from the Euratom research and training programme 2014-2018 under grant agreement No 633053. The views and opinions expressed herein do not necessarily reflect those of the European Commission.

This document is intended for publication in the open literature. It is made available on the clear understanding that it may not be further circulated and extracts or references may not be published prior to publication of the original when applicable, or without the consent of the Publications Officer, EUROfusion Programme Management Unit, Culham Science Centre, Abingdon, Oxon, OX14 3DB, UK or e-mail Publications.Officer@euro-fusion.org

Enquiries about Copyright and reproduction should be addressed to the Publications Officer, EUROfusion Programme Management Unit, Culham Science Centre, Abingdon, Oxon, OX14 3DB, UK or e-mail Publications.Officer@euro-fusion.org

The contents of this preprint and all other EUROfusion Preprints, Reports and Conference Papers are available to view online free at http://www.euro-fusionscipub.org. This site has full search facilities and e-mail alert options. In the JET specific papers the diagrams contained within the PDFs on this site are hyperlinked

On the role of finite grid extent in SOLPS-ITER edge plasma simulations for JET H-mode discharges with metallic wall

S.Wiesen[a], S.Brezinsek[a], X. Bonnin[b], E. Delabie[c] L. Frassinetti[d], M. Groth[e], C. Guillemaut[f], J. Harrison[g], D.Harting[g], S. Henderson[g], A. Huber[a], U. Kruezi[b], R. A. Pitts[b], M. Wischmeier[h] and JET contributors[*]

EUROfusion Consortium, JET, Culham Science Centre, Abingdon, OX14 3DB, UK

[a]Forschungszentrum Jülich GmbH, Institut für Energie- und Klimaforschung – Plasmaphysik, 52425 Jülich, Germany

[b]ITER Organization, Route de Vinon sur Verdon, CS90 046, 13067 St Paul Lez Durance, Cedex, France

[c]Oak Ridge National Laboratory, Oak Ridge,Tennessee 37831-6169, USA

[d]Association VR, Fusion Plasma Physics, KTH, SE-10044 Stockholm, Sweden

[e]Aalto University, Espoo, Finland

[f]Instituto de Plasmas e Fusão Nuclear, IST, Univ. de Lisboa, P-1049-001, Lisboa, Portugal

[g]CCFE, Culham Science Centre, Abingdon OX14 3DB, UK

[h]Max-Planck-Institut für Plasmaphysik, 85748 Garching bei München, Germany

Abstract

The impact of the finite grid size in SOLPS-ITER edge plasma simulations is assessed for JET H-mode discharges with a metal wall. For a semi-horizontal divertor configuration it is shown that the separatrix density is at least 30% higher when a narrow SOL grid width is chosen in SOLPS-ITER compared to the case for which the SOL grid width is maximised. The density increase is caused by kinetic neutrals being not confined inside the divertor region because of the reduced extent of the plasma grid. In this case, an enhanced level of reflections of energetic neutrals at the LFS metal divertor wall is observed. This leads to a shift of the ionisation source further upstream which must be accounted for as a numerical artefact. As a consequence, with a too narrow grid the in/out asymmetry in the neutral pressure usually seen in H-mode experiments cannot be reproduced. Additionally, an overestimate in the cooling at the divertor

[*] See the author list of "Overview of the JET results in support to ITER" by X. Litaudon et al., Nuclear Fusion 57 (2017) 102001

entrance is observed in this case, identified by a reduced heat flux decay parameters λ_q^{div}. Otherwise and further upstream the mid-plane heat decay length λ_q^{up} parameter is not affected by any change in divertor dissipation. This confirms the assumptions made for the ITER divertor design studies, i.e. that λ_q^{up} is essentially solely set by the assumptions for the ratio radial to parallel heat conductivity.

PACS: 52.30.Ex, 52.40.Hf, 52.55.Fa, 52.55.Rk, 52.25.-b

1 Introduction

The prediction of particle and power exhaust for ITER relevant conditions (high-power H-mode, high-density with a partially detached metal-wall divertor) requires validated edge plasma models [1]. SOLPS-ITER [2, 3] includes a state-of-the-art transport model including plasma drifts and improved molecular kinetics, i.e. model features required to quantify a detached divertor operational regime. Over the past few years, 2D edge plasma codes have shown to be incrementally reliable especially for the case of metal devices [4]. The SOLPS-ITER code has been selected by the IO (ITER Organization) as the design tool to predict ITER divertor conditions. With the only exception of [5] the new SOLPS-ITER code is still required to demonstrate that it can reproduce H-mode edge plasma conditions in increased size metal divertors. Modelling exercises like this should demonstrate that the basic assumptions made for the ITER divertor design with metal wall are consistent with present understanding of the physics involved (e.g. turbulent-advective transport or neutral kinetics).

Apart from fundamental unknown modelling parameters like the level of anomalous transport in H-mode discharges, a typical model setup of SOLPS-ITER requires a specific choice of numerical parameters, like the time-step, the level of geometric complexity or an assumption for the grid resolution and its extent. There is some freedom in these numerical parameters as for the given case it is not obvious what the most adequate parameters would be. Often the parameters are chosen more for convenience, for example to simplify the physics model or to achieve numerical convergence as quickly as possible. Sometimes, the modeller is tempted to oversimplify the model setup that neglect, unknowingly, some important aspects of the physics behind.

For example, a typical edge modeller usually choses a SOL grid width that is at least wide enough to include the near-SOL heat decay length parameter λ_q. Sometimes there are also

technical constraints that would not allow a SOL grid width to be wide enough to fully include λ_q and then one possible "workaround" is to reduce the level of complexity for the wall geometry (by removing or modifying edges and corners that would otherwise limit the SOL grid width). As we will show in this paper, such simplifications can have a significant impact on the overall numerical plasma solution. The interpretation of the model results in terms of physics can therefore be hampered, perhaps unknowingly. In this paper we discuss systematically the impact of a finite grid size (i.e. the SOL grid width) and the significance of the level of divertor geometric details on the overall SOLPS-ITER edge plasma solution.

A set of JET H-mode discharges with the ITER-like wall (ILW, tungsten PFCs in the divertor, beryllium for the main-chamber) has been selected for modelling the inter-ELM phase. In the following subsection the experimental setup of the JET discharge is described and the SOLPS-ITER model setup is briefly sketched. The modelling results are presented and compared to the experimental data in section 3. A discussion follows in section 4 highlighting the question of interpretation of model results if one modifies fundamental numerical parameters in SOLPS-ITER like the SOL grid width or geometric details. Section 5 concludes the paper with a summary.

2 Experiment and Model Setup

As experimental basis for the presented numerical exercise well diagnosed JET-ILW H-mode experiments in unseeded conditions from the C30C JET campaign in 2012 had been chosen [6]. In this specific JET campaign a large number of identical plasmas in semi-horizontal divertor configuration had been repeated (Ip/Bt=2.0MA/2.4T, low-δ, P_{NBI}=11MW, deuterium feed-forward gas injection $1.0 \cdot 10^{22}$ s^{-1} into the HFS divertor) to achieve a total accumulated time of 900s in H-mode at with ΔW_{ELM}~160kJ ELMs at f_{ELM}~30Hz. The well diagnosed edge plasma conditions, for which a post-mortem analysis of the PFCs exists, are currently utilized for the analysis of Be/W transport in JET using the ERO2.0 code [7] requiring modelled background plasmas in 2D from SOLPS-ITER.

In the following, the JET plasma discharge #83712 stands as the reference discharge for the C30C campaign. The EFIT equilibrium was taken from this specific discharge, representing the proxy for all identical discharges from the 2 week period of the C30C JET campaign. Upstream n_e and T_e profiles were taken from coherently averaged high-resolution Thomson scattering profiles (HRTS) across all C30C discharges. For having representative upstream conditions for the inter-ELM phase, only those data points shortly before the ELM event were

taken into account in the averaging (i.e. the last 20-30% of the inter-ELM period). From the attached divertor conditions and with the outer strike line positioned on the LFS horizontal target (c.f. fig.1) the evolution of surface temperature T_{surf} and perpendicular target heat fluxes q_{perp} were coherently averaged from the divertor IR camera (IRTV) system (again across all ELMs and discharges from C30C). Also the HFS recycling flux was measured from Langmuir probes averaged coherently and cross-checked with D_α & D_2 molecule spectroscopy. For further analysis of the inter-ELM phase the ELM transients have been removed in the signals (c.f. [8] for an in-depth analysis of the ELM-phase itself in C30C).

The SOLPS-ITER code [2, 3] had been set up for a D-only single fluid plasma simulation with parallel transport (along field lines) assumed to be classical Spitzer with flux limiting corrections applied for electron heat and ion viscosity. Anomalous transport parameters were set to be spatially varying, including an edge transport barrier (ETB) represented by reduced particle diffusion and heat conductivities inside a narrow layer just inside the separatrix. The exact form of the transport parameter profiles for diffusion D_{edge} and heat conductivities $\chi^{e,i}_{edge}$ had been chosen by executing a fitting procedure to match the n_e and T_e pedestal profiles as well heat decay parameter in the near-SOL region upstream. For the latter a slight extension of the ETB into the SOL region was required (~0.4cm). In the far-SOL transport was assumed to be comparably high with no spatial variation. Inside the divertor transport was assumed to be flat at increased level. In the current version of SOLPS-ITER the plasma is not in direct contact with the outer wall, hence a decay length of 3cm was assumed for the plasma boundary conditions at the outer plasma grid edge. A quadratic correction for ballooning transport (increasing with major R) was included. Neither radial pinch-like convection nor drift effects were included in the present study. Boundary conditions were set to correspond to experimental values for heating at the core boundary and the gas-fueling rate into the HFS private flux zone was the same as in the experiment.

To assess the role of the grid size three different geometries had been setup (c.f. fig. 2): case A) a grid with a regular, more narrow width of the SOL region technically limited by a small step-like structure of the LFS horizontal divertor plate, case B) the same as A but with a sloped extension of the LFS horizontal plate into the LFS corner region, and case C) a grid with a wide SOL plasma region to maximize the volume covered by the SOL plasma in the main-chamber; this requires the sloped extension of the LFS target plate into the corner as in B. In all 3 cases, the number of poloidal and radial cells had been kept constant, leading to a somewhat higher radial resolution of the grid in the SOL region for case A and B compared to

C. For all 3 cases the radial grid extent of the SOL at the outer-midplane is large enough to cover at least one heat decay length λ_q.

For the neutral transport modelled by EIRENE, an unstructured triangular mesh was overlaid on top of the plasma grid with each plasma cell being divided up into at least two triangular cells. One of the SOLPS-ITER options is the possibility to extend the triangular mesh for the neutrals into the remote regions in the poloidal plane. This is of specific importance as for JET the only accessible pressure gauge for matching the neutral pressure (an important model constraint [4]) is deep in the sub-divertor region. Also, small structures in the JET's louvre regions can be adequately represented (c.f. fig 3), leading to a significantly reduced flux of energetic atoms towards the pump region in the LFS as in the experiment. With the extended neutral grid option the pump structure itself and its pumping speed can be included in the model as well. The neutral physics model corresponded to the set of atomic and molecular database as generally described in [9]. However, with the divertor in attached conditions neutral viscosity effects could be treated as negligible: for the given attached (low-density) JET simulation case the optional BGK treatment of the neutral viscosity was tested with no dramatic change in the overall result for the plasma profiles (however, the molecular pressure in the divertor increased by a factor ~2 with the neutral viscosity included, c.f. also the discussion section below)

3 Results

In figure 4 the simulation cases are compared with the selected diagnostic data that constrained the model upstream and downstream. Case A has been taken as the first reference for which the profiles have been matched as close as possible to HRTS, Langmuir probe and IRTV data. As explained before the transport model in the other cases B and C are identical to A, with the exception of the grid extent in the SOL and/or geometrical details in the divertor. By taking case A as the reference, the simplified divertor geometry of the divertor (case B) has only a very small impact on the modelled upstream profiles. The existence of the LFS step of the horizontal target plate inside the neutral simulation domain (i.e. a region outside the plasma grid) however leads to a moderate increase of about 15% for target n_e and particle flux Γ_t.

When the width of the SOL grid is widened (case C) a significant decrease in upstream separatrix density n_e^{sep} (30%) is seen, concomitantly with a strong decrease of downstream n_e and Γ_t (65%). As a result of the reduced n_e^{sep} (driven by less neutrals fueling the core region)

the top pedestal density n_e^{ped} is similarly reduced (30%) keeping the density gradient inside the ETB ∇n_e^{ETB} constant. With the pedestal pressure unchanged T_e^{ped} must rise in response to a lower n_e^{ped}. In contrast T_e^{sep} varies much less significantly, a feature of the classical Spitzer's conductivity being not dependent on n_e but $\sim T_e^{5/2}$ and consistent with the two-point model prediction in attached conditions $T_e^{sep} \sim (q_{\parallel} L_c/\kappa_{0e})^{2/7}$, with L_c connection length, κ_{0e} parallel electron conductivity. With the increased ∇T_e^{ETB} the parallel heat flux $q_{\parallel} \sim P^{sep}/R_{maj}$ is increased which leads to a ~65% larger $T_{e,t}$ at the target plate. As a result the total plasma heat load density arriving perpendicular at the LFS target plate $q_{perp,t} \sim \gamma \Gamma_t T_{e,t}$ in case C is similar to case A/B (assuming constant sheath heat transmission factor γ in SOLPS-ITER) and remains also within the ballpark of 15% compared to the peak experimental IR data of $q_{perp,t}$.

For further analysis of the impact of the finite SOL grid width on the target heat flux, the experimental and numerical $q_{perp,t}$ profiles (along the target s-coordinate) have been deconvoluted adopting the Wagner/Eich fitting procedure [10, 11]. Figure 5 summarizes for the investigated cases and additional cases with modified transport and/or pumping albedo R (pumping speed). The values for the heat decay parameter $\lambda_{int}^{div} = \lambda_q^{div} + 1.64 \cdot S$ at the divertor entrance [12] and the numerically derived value for λ_q^{up} from the outer midplane heat flux profiles are compared with the experimentally measured quantities. SOLPS-ITER underestimates (5-25%) λ_{int}^{div} and a dependence on the SOL grid width is observed: λ_{int}^{div} is 20% larger in case C with the wide SOL grid width.

In order to match the upstream profiles also for the wide SOL grid case C, the ETB transport parameters have been modified (decrease of D^{ETB} by ~ factor 2, increase of $\chi_{e,i}^{ETB}$ by 15%, reduction of pumping speed (1-R) by ~ factor 3). In the following, this amended case is named as case C^*. For the cases in which the upstream conditions/profiles for n_e and T_e are matched (cases A, B and C^*) it is obvious that λ_q^{up} is barely affected by the divertor conditions: neither the SOL grid width nor a change in the pumping speed contribute to a change to λ_q^{up}. It is solely the transport assumption for the radial heat conduction which sets λ_q^{up} upstream.

Compared to the wide SOL grid case C/C* an extra cooling of the SOL further downstream is observed in case A/B with the narrow SOL grid width being reflected by a reduced ratio $\lambda_{int}^{div}/\lambda_q^{up}$ in case A/B (c.f. fig 5).

The radial particle fluxes towards the outer wall are also affected by the SOL grid width (c.f. fig 6). With the narrow grid (case A/B) the fluxes towards the wall are enhanced by a factor 4-5 compared to the wide grid case C. With the decay length fixed at the outer boundary the change in flux must be purely attributed to a proportionally change in the plasma density in the far-SOL. The re-matched case C^* with modified transport/pumping speed lies somewhat in between the two extremes.

4 Discussion

The observations from above can be relatively easy contributed to a change in the neutral distribution when moving from the wide towards the narrower SOL grid width. For the latter (case A/B) neutrals can move more freely across the far-SOL region in the LFS region and may even reach the LFS baffle region above the divertor. From molecular pressure p_{D2} estimates from the model (c.f. fig. 7) the narrow SOL assumption is not able to compress the neutrals significantly in the LFS. Whilst in the wide SOL grid case (case C) the LFS pressure close to the louvre region is about ~2 larger compared to the HFS louvre, the pressure in cases A/B becomes quite in/out symmetric. Unfortunately, at JET the pressure gauge coverage inside the divertor is practically not existing and the in/out asymmetry in the neutral pressure cannot be compared directly to the experiment. The only sub-divertor pressure gauge measurement available gives pressures way below the expected range of pressure of the order of 1 Pa (c.f. fig. 7). Whereas the modelled neutral pressure inside the divertor resides in the right ballpark (as it is largely determined by the gas puff and thus an engineering parameter, c.f. [13]) the experimental value in the sub-divertor gives a one order of magnitude lower value for the molecular pressure. Such a strong loss in p_{D2} between the upper sub-divertor region and the pressure gauge was not expected by the authors, and is currently not seen in the model too. For further assessment the calibration of the sub-divertor pressure was double-checked and the authors conclude that the measurement was correct. The discrepancy the sub-divertor pressure values for p_{D2} is possibly linked to an overestimate in the neutral conductivity through the louvre structures and hence a too large molecular flux into the sub-divertor. This is possibly also correlating to the fact that for the numerical pumping speed at the cryo-pump was required to be larger than to the nominal value ~200 m^3/s. A numerical assessment is currently ongoing (extending the work done by Varoutis and Bonelli in [14, 15]) in order to identify which of the following neutral transport parameters need to be furtherly constrained: neutral viscosity (BGK option in EIRENE), neutral conductance

through the louvres, temperature of walls (thermalizing neutrals). The result of this assessment are to be presented in a future paper.

The narrow SOL grid model assumptions not only produce a quantitative change (lower LFS neutral compression) but also a qualitative change in neutral transport is observed. With no plasma in the way, fast atoms can be easily reflected off the outer vertical divertor plates and hence reach (more indirectly) the region above the X-point. Figure 8 displays for the narrow and wide grid case a comparison of the ionization source clearly showing the qualitative difference between both cases. With the neutrals being able to be transport further upstream the SOL in the narrow grid case the ionization of particles further upstream requires the energy that leads to a reduction of the $\lambda_{int}^{div}/\lambda_q^{up}$ ratio (with λ_q^{up} staying constant and essentially set by mid-plane transport assumptions).

In the overall particle balance the ionized particles further upstream are partially transported outwards towards the wall, explaining the 4-5 larger wall flux in case of the narrow SOL grid assumption.

5 Conclusions

It has been demonstrated that for the modelling of the edge plasma conditions for the inter-ELM phase in JET type-I ELMy H-mode discharges with Be/W wall the impact on the finite grid size (i.e. the SOL grid width) cannot be ignored. Especially for more open divertor geometries (i.e. the semi-horizontal divertor configuration) and assuming a too narrow SOL grid width the LFS neutral compression can be significantly underestimated leading to a symmetric in/out neutral pressure equilibration. With the neutrals finding a kinetic transport path that increases the particle source further upstream, the heat flux width at the divertor entrance becomes wider due to increased cooling leading to a reduction of the $\lambda_{int}^{div}/\lambda_q^{up}$ ratio. Concomitantly, the mid-plane value of λ_q^{up} stays always the same and is set by the ratio of radial to parallel conductivities at the mid-plane. By keeping all other transport parameters identical, the SOL grid not extending up closer to the wall leads to significantly reduced upstream densities inside the pedestal region and at the separatrix (30% reduction in n_e^{sep}). In such conditions it is possible to increase the density at separatrix and inside the pedestal by modifying numerically the assumption for transport and recycling. However, due to the arbitrariness in such a re-fitting procedure the understanding of the physics (transport, fueling, recycling etc) becomes blurred. It is obvious that the physics interpretation of the numerical results are subject to the possibility of the modeler's ignorance to the finite grid size issue.

For example, providing input to wall erosion codes like ERO2.0 [7] it is the radial outflow towards the main wall that becomes increased by at least a factor 4-5 if the grid is not extended. The results shown suggest that for calculating the numerical error in the computation of wall erosion fluxes the difference between the two extreme cases (narrow and wird SOL grid width) should be taken as a guideline to estimate the validity of the background plasma.

In the near future, SOLPS-ITER will have the option of extending the plasma grid up to the actual main wall (and down into the regions of the private flux zone, too). This is still work in progress and comes with a modification of the boundary condition assumption at the wall towards more realistic conditions other than simply radial decay lengths, taking into account the actual sheath physics also for the case with glazing angles. Because of the low divertor densities in the investigated H-mode JET discharges, the neutral viscosity does not play a large role and it was shown that small modifications in the divertor wall geometry (e.g. inclusion of a small step in the LFS target plate) only have a minor impact on the overall plasma solutions. It is expected however that with extended grid feature in SOLPS-ITER and/or at higher densities the details in the actual divertor wall structure can be more significant, especially if the simulated (far-SOL) plasma itself is in direct contact with steep edges in the poloidal target tile configuration.

ITER will have a more closed divertor configuration compared to the JET discharge discussed above with strike-lines on both low and high-field side vertical target plates. ITER will operate at higher density with the divertor in a strongly dissipative regime and having partially detached conditions at the LFS divertor induced by Ne or N impurity seeding. Neutral viscosity does also play a role in at elevated densities [16] and the geometric details do matter for the calculating the neutral conductance towards the pump. For ITER relevant edge plasma conditions, an additional study on the impact of the grid size and resolution for N-seeded H-mode JET discharges are currently under way (Ip/Bt=2.5MA/2.7T at P_{NBI}=20MW in partial detached conditions with a radiated fraction of ~45%, c.f. [17]). The results of this, numerically demanding, exercise (with a fluid time step < 10^{-6} s) will be presented elsewhere. However, first indications from the ongoing modelling of this JET discharge show that the neutrals in such a closed vertical divertor configuration are much more compressed and any remaining neutral leakage is more related to neutral pathways behind remote areas (c.f. also the work from [5] for Alcator C-mod). In turn the ionization source is kept well inside the divertor volume, closer to the target plates. It is therefore

expected that the assumption of λ_q^{up} being essentially set by the ratio of radial to parallel heat conductivities at the mid-plane is always a good approximation also for ITER.

All simulations presented here for JET have not been taking into account drift flows. From the experience of modelling of other devices the combined grad-B and ExB drifts leads to a rotation of the flows in clock-wise direction (having the grad-B drift pointing towards the lower divertor). It is expected that by including drift effects the sustained the neutral compression asymmetry (for the wide grid case C a factor ~ 2 in the LFS divertor compared to the HFS divertor) will be somewhat amended leading to a more in/out symmetric neutral pressure distribution. By the time of writing of this paper new H-mode JET simulations including drifts (unseeded conditions for the C30C campaign) are being set up, with the results to be presented elsewhere in the future.

Acknowledgements

This work is in the context of a wider SOLPS-ITER modelling activity towards ITER scale and within the projects done for the ITER Scientist Fellow Network (ISFN). The views and opinions expressed herein do not necessarily reflect those of the ITER Organization. This work has been carried out within the framework of the EUROfusion Consortium and has received funding from the Euratom research and training programme 2014-2018 under grant agreement No 633053. The views and opinions expressed herein do not necessarily reflect those of the European Commission.

References

[1] M. Wischmeier, *J. Nucl. Mat.,* vol. 415, p. S523, 2011.

[2] S. Wiesen, *J. Nucl. Mat,* vol. 415, p. 480, 2015.

[3] X. Bonnin, *Plasma and Fusion Research,* vol. 11, p. 1403102, 2016.

[4] S. Wiesen, *Nucl. Mater. and Energy,* vol. 12, p. 3, 2017.

[5] W. Dekeyser, *Nucl. Mater. and Energy,* vol. 12, p. 899, 2017.

[6] S. Brezinsek, *Nucl. Fusion,* vol. 53, p. 083023, 2013.

[7] J. Romazanov, "this conference".

[8] S. Wiesen, *Nucl. Fusion,* vol. 57 , p. 066024, 2017.

[9] V. Kotov, *Plasma Phys. Control. Fusion,* vol. 50, p. 105012, 2008.

[10] F. Wagner, *Nucl. Fusion,* vol. 25, p. 525, 1985.

[11] T. Eich, *Nucl. Fusion,* vol. 53, p. 093031, 2013.

[12] M. Makowski, *Phys. Plasmas,* vol. 19, p. 056122, 2012.

[13] A. Kallenbach, "this conference".

[14] S. Varoutis, *Fus. Eng. Des.,* vol. 121, p. 13, 2017.

[15] F. Bonelli, *Nucl. Fusion,* vol. 57, p. 066037, 2017.

[16] A. Kukushkin, *Fusion Eng. Des.,* vol. 86, p. 2865, 2011.

[17] M. Wischmeier, in *Proc. IAEA-FEC*, Kyoto, Japan, 2016.

Figure captions

Figure 1: Semi-horizontal divertor geometry setup of JET discharge #83712 representing a reference to all discharges executed during the C30C campaign.

Figure 2: The three different grid cases. The red grid represents the structured quadrangular plasma grid in SOLPS-ITER. Overlaid (in black) is the unstructured triangular mesh for the neutrals (EIRENE) including the cells for the plasma cells, each split into 2 triangles. Unlike the plasma grid the neutral triangular mesh is touch the outer wall.

Figure 3: The full unstructured triangular mesh including the structures for the sub-divertor, the louvre structures, the pump and puff location as well as the location of the single pressure gauge well below the divertor region.

Figure 4: Comparison of up- and downstream profiles experiment vs. model. The color code is as in fig.2 and represents the plasma grid variation and modification sin the divertor structure: case A narrow SOL grid width with step in LFS target plate (yellow), case B narrow SOL grid width with stretched LFS target slope (red) and case C wide SOL grid width that technically requires the LFS target to be sloped (blue).

Figure 5: Comparison of experimental (IRTV) and modelled heat flux parameters by using the Wagner/Eich fitting procedure at divertor entrance λ_q^{div} (neglecting flux expansion) and diffusion parameters S, and the heat decay length directly taken from the mid-plane location λ_q^{up}. The three cases on the right are those cases with matched upstream profiles to the experiment (HRTS), namely case A (yellow), B (red) and C* (purple, c.f. text). The other cases in the middle are scans for recycling coefficient R or modifications in transport. The marked case C (blue) represents the case without any modifications to case A/B but the SOL grid width.

Figure 6: Radial plasma outflow towards the walls (taken at the outermost plasma grid boundary not directly in touch with the walls), Color code as in fig. 2 for cases A, B, C and C* (with the re-matched case C* in purple).

Figure 7: Modelled molecular pressure p_{D2} at the inner and outer divertor louvre regions, and at the location of the sub-divertor pressure gauge. For comparison the experimental value for the sub-divertor pressure is shown too, showing a massive discrepancy (one order of magnitude) to the modelled p_{D2} (c.f. discussion in text).

Figure 8: Left: total ionization source for case A, right: the same for case C. For case A the typical kinetically reflected pathways for neutrals are sketched, leading to a decrease in the neutral confinement at the LFS and balancing out of in/out neutral pressures. In case A the particle source is enhanced further upstream at the divertor entrance, leading to a stronger cooling in that region compared to case C.

Figure 1

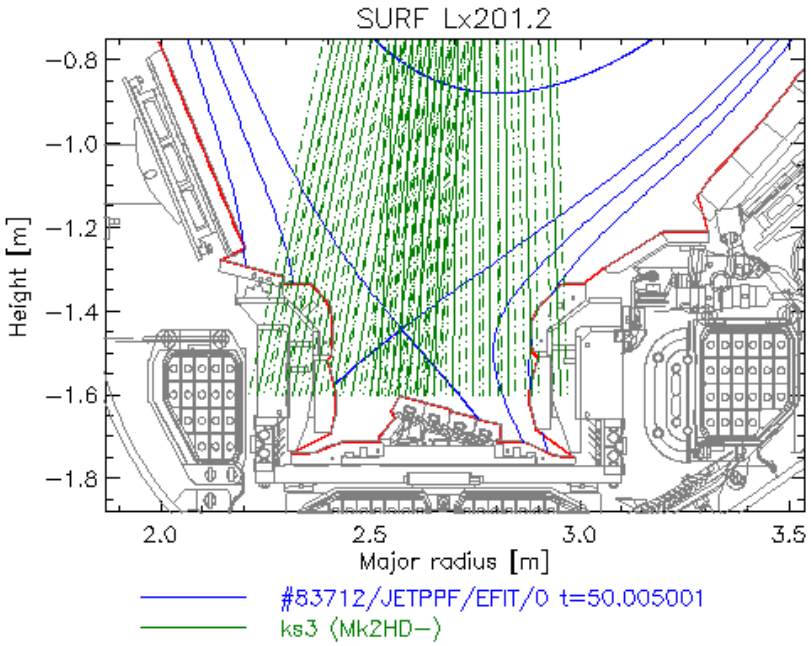
SURF Lx201.2
−0.8
−1.0
−1.2
−1.4
−1.6
−1.8
Height [m]
2.0
2.5
3.0
3.5
Major radius [m]
#83712/JETPPF/EFIT/0 t=50.005001
ks3 (Mk2HD−)

Figure 2

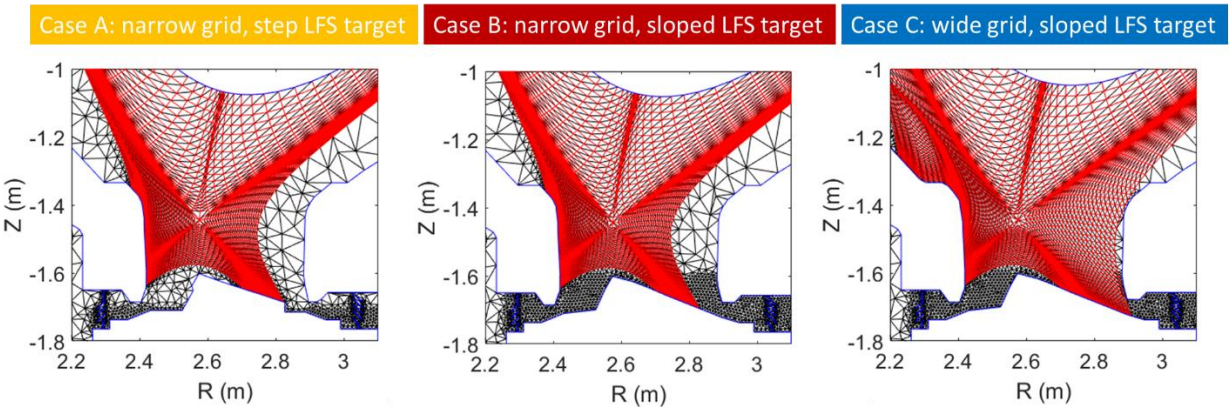
Case A: narrow grid, step LFS target
Case B: narrow grid, sloped LFS target
Case C: wide grid, sloped LFS target
Z (m)
-1
-1.2
-1.4
-1.6
-1.8
2.2
2.4
2.6
2.8
3
R (m)

Figure 3

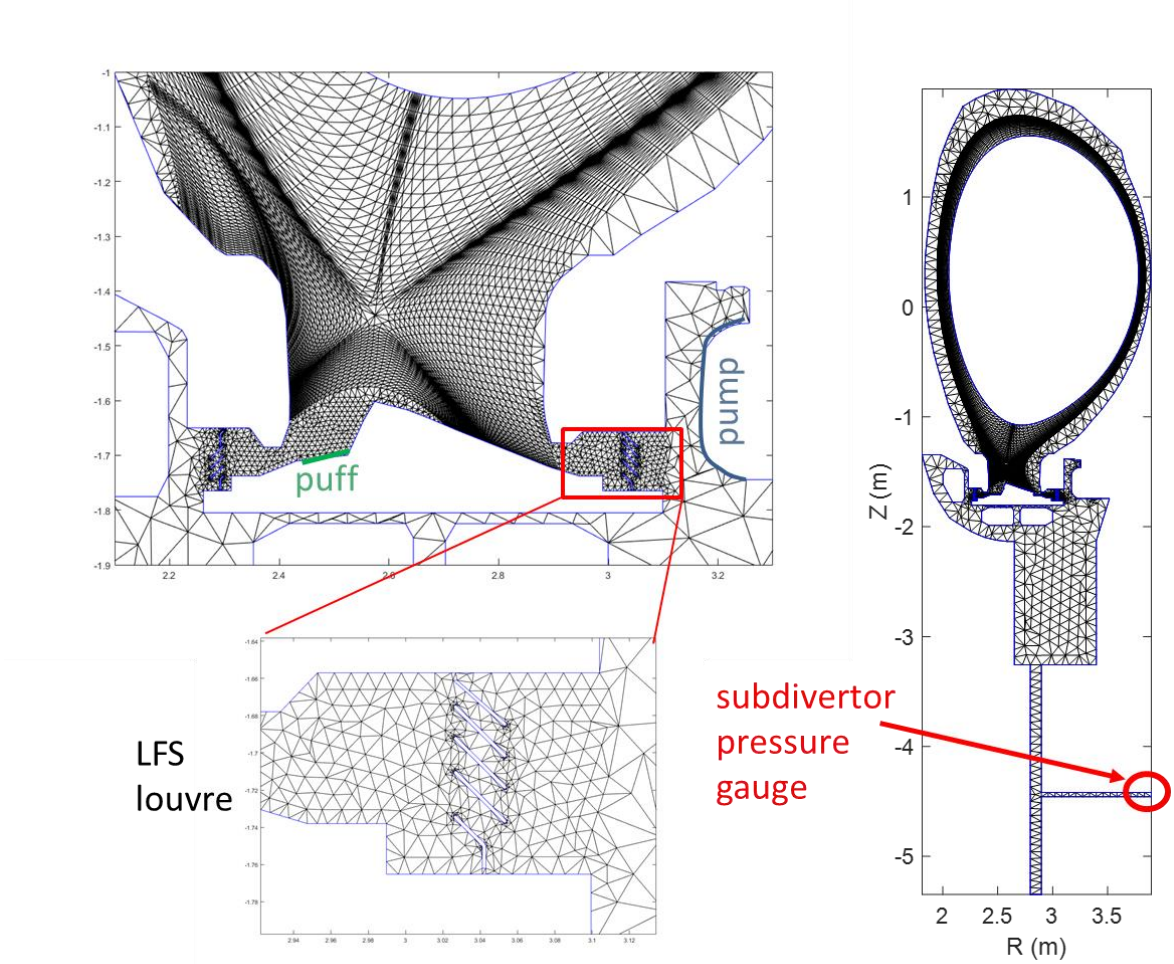
puff
pump
LFS
louvre
subdivertor
pressure
gauge
Z (m)
R (m)
1
0
-1
-2
-3
-4
-5
2
2.5
3
3.5

Figure 4

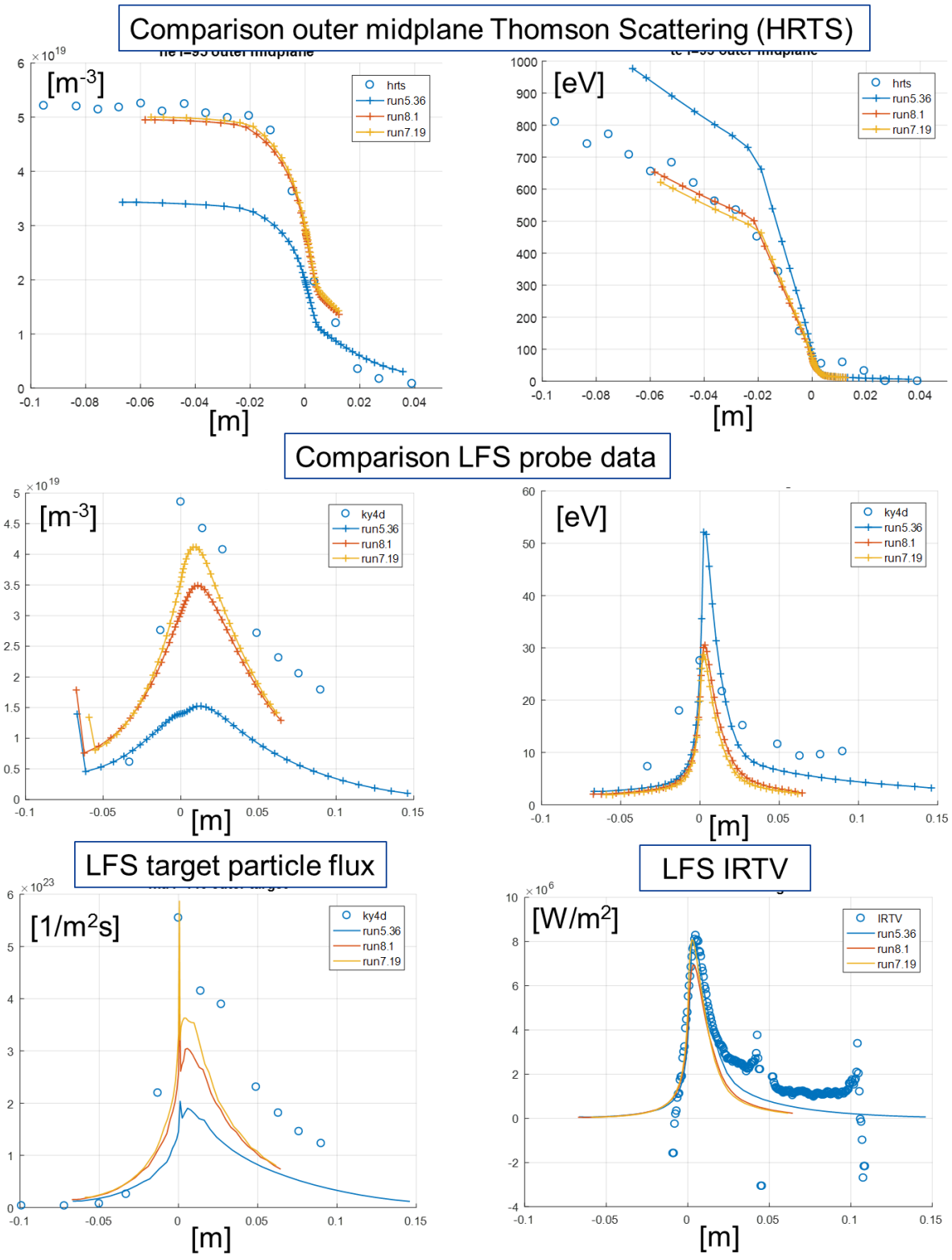
Comparison outer midplane Thomson Scattering (HRTS)
[m-3]
[eV]
hrts
run5.36
run8.1
run7.19
[m]
Comparison LFS probe data
ky4d
LFS target particle flux
[1/m2s]
LFS IRTV
[W/m2]
IRTV

Figure 5

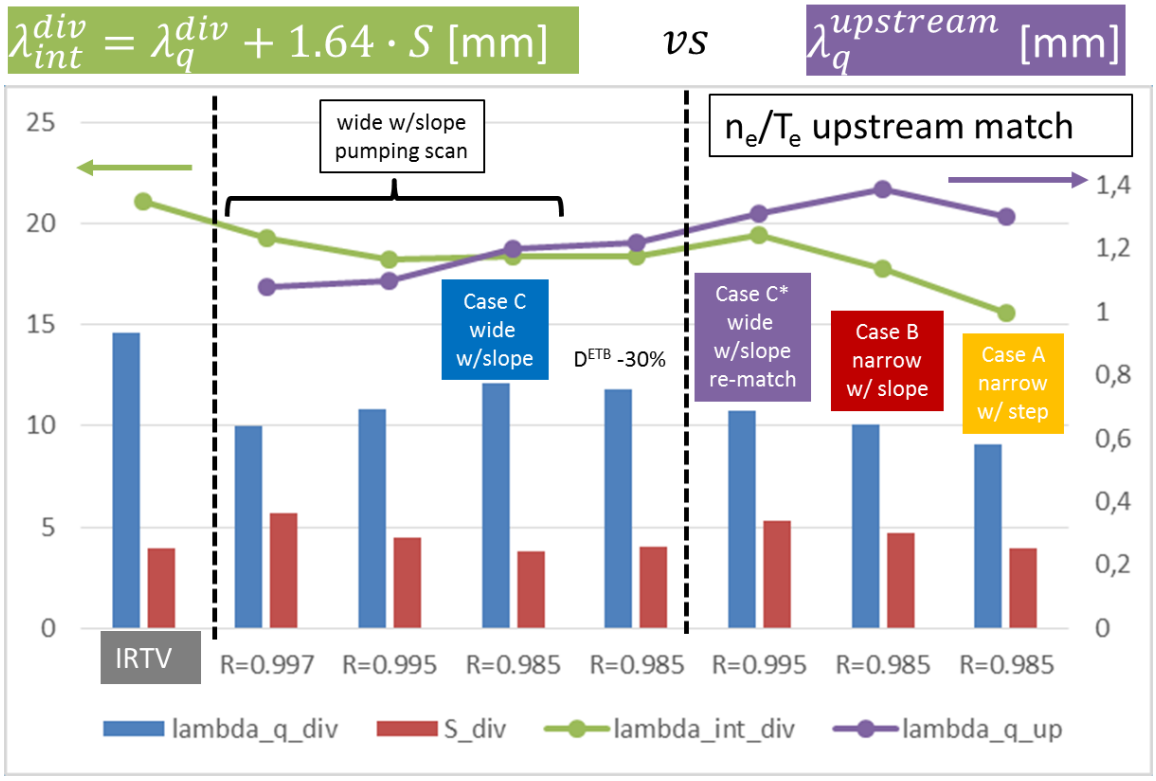
$\lambda_{int}^{div} = \lambda_q^{div} + 1.64 \cdot S$ [mm]
vs
$\lambda_q^{upstream}$ [mm]
wide w/slope pumping scan
n_e/T_e upstream match
Case C wide w/slope
D^{ETB} -30%
Case C* wide w/slope re-match
Case B narrow w/ slope
Case A narrow w/ step
IRTV
R=0.997
R=0.995
R=0.985
R=0.985
R=0.995
R=0.985
R=0.985
lambda_q_div
S_div
lambda_int_div
lambda_q_up

Figure 6

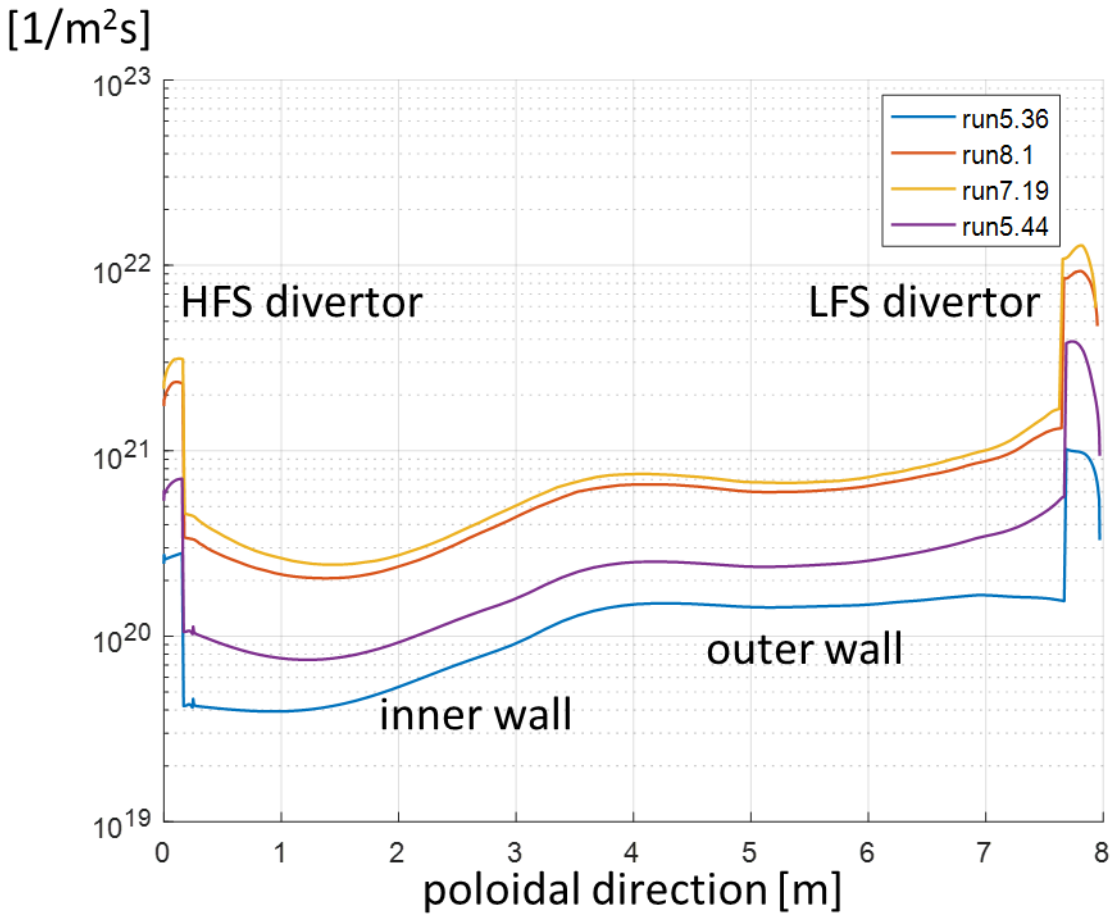
[1/m²s]
10²³
10²²
10²¹
10²⁰
10¹⁹
0
1
2
3
4
5
6
7
8
poloidal direction [m]
run5.36
run8.1
run7.19
run5.44
HFS divertor
LFS divertor
outer wall
inner wall

Figure 7

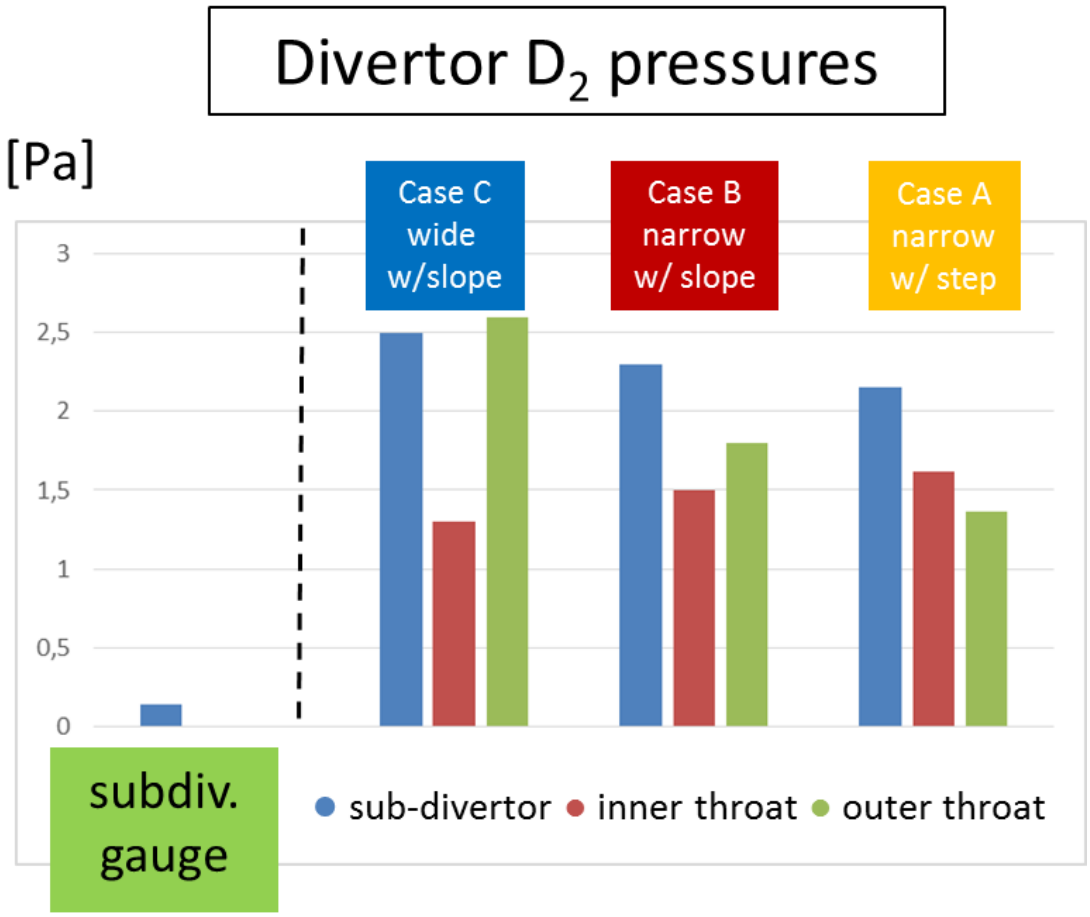
Divertor D_2 pressures
[Pa]
Case C wide w/slope
Case B narrow w/ slope
Case A narrow w/ step
3
2,5
2
1,5
1
0,5
0
subdiv. gauge
sub-divertor
inner throat
outer throat

Figure 8

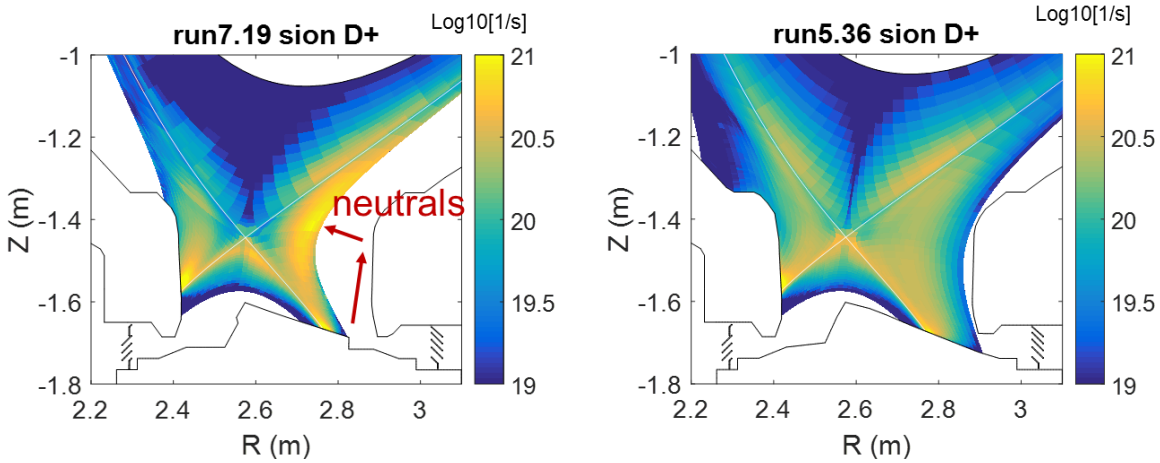
run7.19 sion D+
Log10[1/s]
neutrals
Z (m)
R (m)
-1
-1.2
-1.4
-1.6
-1.8
2.2
2.4
2.6
2.8
3
21
20.5
20
19.5
19
run5.36 sion D+
Log10[1/s]
Z (m)
R (m)